Alexandria Engineering Journal (2021) 60, 3649–3667

HOSTED BY

ELSEVIER

Alexandria University

Alexandria Engineering Journal

www.elsevier.com/locate/aej
www.sciencedirect.com



Numerical and experimental investigation of fuel consumption and CO_2 emission performance for a parallel hybrid vehicle



Özgün Balcı [a,*], Yasin Karagöz [b], Onur Gezer [a], Sefa Kale [a], Hasan Köten [b], Saban Pusat [a], Levent Yüksek [a]

[a] Department of Mechanical Engineering, Yildiz Technical University, Yildiz, Istanbul 34349, Turkey
[b] Department of Mechanical Engineering, Istanbul Medeniyet University, Istanbul 34000, Turkey

Received 26 July 2020; revised 31 January 2021; accepted 14 February 2021

KEYWORDS

Parallel hybrid vehicle;
Hybrid system;
Vehicle model;
Emission;
Fuel consumption

Abstract In this study, fuel consumption map was created by obtaining a large number of data from gasoline engine passenger car through high-speed data acquisition with ISO-15765–4-CAN Protocol. Subsequently, CO_2 map was also generated theoretically. To obtain precise results, ANN was used while creating the maps. Later, conventional vehicle model was created with Matlab/Simulink. Afterwards, hybrid vehicle model was developed by implementing electrical system in compliance with single-shaft pre-transmission parallel configuration with one electric motor. Hybrid powertrain control algorithm was created by considering efficiencies of mechanical and electrical power sources and sinks. Charge-neutral simulations were run with conventional and hybrid models over WLTC and a local route which is created by collected in-city speed data. The hybrid and conventional vehicles were enabled to be compared with the developed method. Detailed comparison of ICE operations both between two vehicle models and two cycles was presented. Moreover, obtained results, including overall electrical system efficiencies, were compared over WLTC and the local route. Significant improvements both in consumption and CO_2 values were concluded. It is also concluded that using the hybrid system in local route with higher proportion of in-city driving conditions caused higher improvements despite a slight decrease in overall electrical system efficiency.

© 2021 THE AUTHORS. Published by Elsevier BV on behalf of Faculty of Engineering, Alexandria University. This is an open access article under the CC BY-NC-ND license (http://creativecommons.org/licenses/by-nc-nd/4.0/).

1. Introduction

Daily consumption of petroleum products is 60,000,000 barrels due to the exceeding a billion vehicles [1]. Transportation sourced exhaust emissions, which are progressively restricted by authorities, cause increasing of environmental pollution

* Corresponding author.
E-mail address: obalci@yildiz.edu.tr (Ö. Balcı).
Peer review under responsibility of Faculty of Engineering, Alexandria University.

https://doi.org/10.1016/j.aej.2021.02.025
1110-0168 © 2021 THE AUTHORS. Published by Elsevier BV on behalf of Faculty of Engineering, Alexandria University.
This is an open access article under the CC BY-NC-ND license (http://creativecommons.org/licenses/by-nc-nd/4.0/).

especially in residential areas. In order to fulfill the demanding emission regulations, a significant amount of attempts were conducted on advanced emission reduction devices and strategies, and vehicle electrification. Electrification of vehicles is focused on pure electric vehicles (PEVs) and hybrid electric vehicles (HEVs). PEVs emit zero tail pile emission [2]. However, the eco-friendly behavior of electrical vehicles differ based on electricity production methods. PEVs need big and heavy batteries and power suppliers to reach sufficient ranges [3]. HEVs are favorable in terms of environment and commercialization, considering the source of electrical energy, vehicle mass growth and battery capacity problems with compared to PEVs. PEVs generally require 20 kWh battery capacity, while this value is reduced to 2 kWh in HEVs [4]. The popularization of HEVs presents rational, practical and realistic solutions to reduce the fuel consumption and ensure the emission regulations. For the NEDC cycle, permitted CO_2 emission value targets for passenger car vehicles are 95 g/km for 2021, which is 27% and 50% lower than the 2015 and 2010 levels, respectively [5].

Three common types of HEV configurations are series, parallel and series–parallel [6]. In parallel hybrid systems, the traction power and torque, which are produced by the internal combustion engine (ICE), can be transmitted directly to the drive wheels. Electric motor (EM) works as a supporting unit transiently or continuously, especially under sudden power and torque requirements. Sometimes, motor works as a single drive unit at extremely inconvenient region of the ICE. Parallel hybrid applications are preferred mostly for light duty and passenger cars, they can accommodate one or more electric motors [6]. Both of ICE and motor can be chosen with smaller capacity due to the supporting role of the motor in parallel HEVs. Therefore, parallel HEVs are advantageous in terms of fuel economy compared to serial hybrid [7], owing to reduction of vehicle mass.

The greatest advantage of HEVs is operating of ICE at more efficient zones, while maintaining potential of regenerative braking [8]. The torque and efficiency of the internal combustion engine are strongly dependent on the engine speed and load. Contrary, the electric motor is more unresponsive in terms of speed and torque differences [4]. The speed-related efficiency reduction for motors is relatively low, especially at high rotational speed regions [9].

Some studies in the literature, which were conducted on HEVs, are presented as follows.

Tribioli and Bella [10] investigated emission and fuel consumption behavior of parallel HEVs. They found 50% emission and 35% fuel consumption reduction. Millo et al. [11] carried out an experimental and simulation based study on light duty commercial diesel vehicles. They observed 23% decrease in CO_2 emission for the NEDC cycle. However, these two studies were performed for plug-in parallel HEVs. It's hardly possible to observe such a high decrease at non-plug-in HEVs. So the studies conducted on non-plug-in HEVs are presented in the following paragraphs.

Taymaz and Benli [12] investigated CO_2 emissions for different fuel types and volume of engines in comparison with hybrid application and conventional type. According to the simulation results, a significant decrease in CO_2 emissions was observed in hybrid applications compared to conventional applications. The fuel consumption values decreased for both gasoline and diesel fueled cases, despite extra weight of additional units.

Al-Samari [13] carried out a study for 110 kW gasoline engine and generator assisted parallel HEV with the same ICE. As a result of the study, the average ICE efficiency during the whole cycle was 23% in the conventional vehicle, the average internal combustion efficiency in the parallel HEV vehicle reached up to 30% during FTP cycle.

Lui et al [1] observed 13.1% reduction in fuel consumption for NEDC cycle and 9.6% reduction in fuel consumption for UDDS cycle in their Matlab based mathematical study with using a parallel HEV instead of a conventional type.

Arat [14] worked on a conventional ICE and its parallel hybrid variation in a part of their own numerical study. They observed higher power output and lower fuel consumption, CO_2 emissions and NO_X emissions for parallel HEV. With regard to the vehicle torque, significant improvements were observed with parallel HEV, especially in terms of conventional drive systems.

Karaoğlan et al. [15] compared conventional vehicle and parallel HEV in their Matlab-Simulink based study. They observed 17% reduction in fuel consumption, 9.1% reduction in CO_2 emission, 18% reduction in CO emission, 4% reduction in HC and 8% reduction for the NO_x release.

Hmidi et al. [16] obtained data for the NEDC cycle in their study on a non-plug-in parallel HEV. In the case of a conventional driving strategy with 1.2 L displacement, gasoline ICE, fuel consumption was 5 L/100 km in the NEDC cycle, this value decreased to 3.86 L/100 km in the non-plug-in parallel hybrid strategy, even with the fuzzy logic controller this value was further reduced up to 3.61 L/100 km.

Garcia et al. [17] studied on a single-shaft parallel HEV model with the engine data obtained according to the gasoline and diesel dual fuel reactivity controlled combustion strategy for WLTC cycle. 5.73 L/100 km fuel consumption, 0.310 g/km NOx emission, $4x10^{-3}$ g/km soot emission were observed under the only ICE propulsion strategy. The hybrid strategy has been evaluated for both control strategies based on fuel consumption and NOx emission control. Fuel consumption based modelled HEV fuel consumption decreased to 4.14 L/100 km, NOx emission increased to 1.36 g/km, soot emissions decreased to $2x10^{-3}$ g/km. NOx controlling based HEV strategy, fuel consumption decreased to 4.72 L/100 km, NOx emission decreased to 0.057 g/km and soot emission $0.6x10^{-3}$ g/km.

Conversion rates between energy forms in parallel HEVs are lower than serial HEVs [18]. Less amount of energy to be lost in energy form conversion processes makes parallel HEVs attractive. Electrically variable transmission is generally preferred in parallel HEVs, such systems have high costs and require two electrical machines [19]. Alternatively, it is possible that, parallel HEVs can be designed as single shaft. In single-shaft systems, the electric machine can perform as both electric motor and generator [20]. Thus, this type of driving system becomes more compact and consists less element. These advantages reduce costs of system, mass of vehicle and increase conversion and mechanical efficiency. Single-shaft hybrid powertrain systems can support five different drive states, these are fully electrically driving, fully ICE driving, hybrid driving, charging and regenerative braking modes [21]. Numerous studies have been conducted on parallel HEVs. Most of these studies are related to plug-in parallel HEVs and they determine large decreases in fuel consumption values. However, energy consumption values and losses occurring

during supply obscure the reliability of the results. For this purpose, non-plug-in parallel hybrid system was preferred in this study. In the literature, generally, the fuel consumption performance of different hybrid strategies have been compared in this field. In addition, the number of studies on single-shaft parallel hybrid systems is quite scarce. The aim of this study is to contribute to the elimination of the deficiencies in this field in the literature by comparing the fuel consumption and CO_2 emissions of a single-shaft, non-plug-in parallel HEV with the conventional ICE vehicle.

In this study, engine maps were created by using the engine data from the sensors via Can Bus protocol by utilizing ANN. Later on, fuel consumption and CO_2 emissions were compared both in WLTC and the chosen route for the single-shaft parallel HEV and conventional gasoline fueled vehicle. The conventional vehicle model was developed by using data from a base vehicle and engine in Matlab-Simulink. The developed vehicle model was revised and adapted for the parallel HEV model. The control strategies, which mainly enables the EM during low power demands, as well as the constraints for the parallel HEV driving system were identified. In order to obtain more realistic results, engine map data obtained experimentally from an engine during drive was used. Thus, CO, HC and NOx data could not be obtained and did not worked in this study. It was concluded that it was possible to generate significant improvements with ICE, compared to conventional gasoline engine, by ensuring the constant positioning of the ICE in the most efficient area on the engine maps during cycles.

2. Modelling

2.1. On-board vehicle engine data acquisition and engine modelling

Test engine is a naturally aspirated, four stroke, conventional gasoline engine, and its specifications are listed in Table 1. Engine fuel consumption data was obtained by implementing a series of test cycles. Fuel consumption maps are generally comprised of two-dimensional, torque-rpm based, brake specific fuel consumption measurements. However, this kind of data is obtained via steady-state tests and is not suitable for dynamic modelling due to various altering inputs during real-driving conditions. In-order to improve the model accuracy, the dynamic tests are implemented. The data were obtained by engine powertrain control module via ISO 15765–4 CAN protocol. Transient behavior of the engine depends on several conditions and the inputs such as load, engine speed, coolant temperature, accelerator pedal position and its differential, knock tendency, ignition timing, altitude, intake air temperature and catalyst efficiency, etc. In addition to these parameters, the powertrain control module adjusts the air/fuel ratio for pre-determined or on-demand conditions. The catalyst heating period or higher acceleration demand conditions are typical examples. The determination of the transient engine behavior is important for developing more precise computer based models, especially for real life based cycle simulations such as WLTC or FTP75. The high speed data acquisition via ISO 15765–4 CAN protocol was established for this model study which has 20 ms refresh rate for all the parameters recorded. Parameters used in the study and structure of the ANN model are summarized in Fig. 1.

Table 1 Specifications of the test engine.

Specification	Value/Description
Aspiration	Naturally aspirated
Number of cylinders/ Configuration	4/inline
Total displacement	1596 cm^3
Compression ratio	11.0
Engine type	Port fuel injection-Gasoline
Engine control	Electronic fuel injection, Closed-loop lambda control with 3-way catalyst, Map based ignition timing control.
Cooling system	Water cooled-thermostat controlled.
Fuel injection pressure	4 bars
Engine power at rated speed	100 hp
Engine torque at rated speed	150 Nm

Accelerator pedal position (APP), engine coolant temperature (ECT), engine speed, intake air temperature (IAT), accessory load, powertrain control module (PCM) state, equivalence ratio, manifold absolute pressure (MAP), air-conditioning state, ambient pressure and fuel injection quantity per cycle are the inputs for the developed ANN model. The outputs of the developed ANN model are fuel consumption, engine load and air inducted by the engine. The input data used in the developed ANN model are collected from a passenger car used in real-life driving conditions and the number of total data points utilized in the ANN model is 1,467,609.

The Matlab software is used in the development of the ANN model. In this study, a well-known feed-forward network is used with two layers as sigmoid hidden neurons and linear output neurons. Levenberg-Marquardt is commonly used on the purposes of internal combustion engine diagnosis [22]. Therefore, Levenberg-Marquardt back-propagation algorithm is used as a training algorithm. Data points are randomly divided into three parts for the ANN model development:

- 70% of the data is used in the training stage (1,027,325)
- 15% of the data is used in the validation stage (220,142)
- 15% of the data is used in the testing stage (220,142)

Two different approaches are employed as the mean squared error and the regression value in the evaluation of the results of the ANN. Some test are conducted to investigate the effect of the neuron numbers, and the number of hidden neurons is selected as 10. In the test, the regression value is obtained in the range of 75%-85% which is very sufficient. There is not a well-accepted procedure to determine the weights between the layers. Therefore, the weights between the layers are determined by trial and error method with relative error evaluation.

For this study, The ANN model is developed to determine the fuel consumption, engine load and air inducted. According to the results, a highly applicable model was developed with overall regression value of 85% which is highly sufficient. The developed model is used to predict the fuel consumption, engine load and air inducted and use in the following parts of the study.

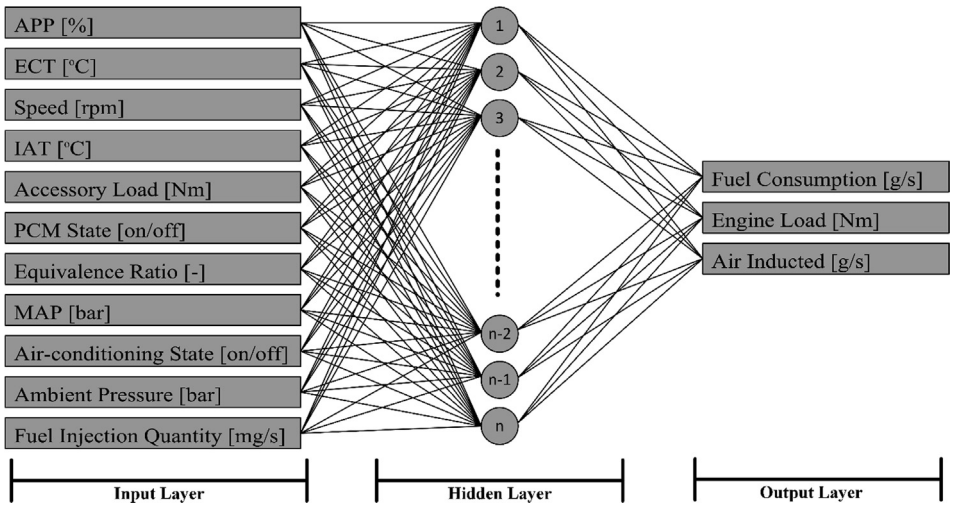


Fig. 1 The ANN structure for this study.

2.1.1. The engine maps

As can be seen from the Fig. 2, the engine maps were created with the engine data obtained through Can Bus protocol with the help of the ANN model. Therefore, engine map providing the brake-specific fuel consumption depending on engine speed and engine torque, were generated. Similarly, the brake-specific CO_2 emission map depending on the engine speed and engine torque were also obtained. The engine maps are used as inputs in the theoretical vehicle models to be created subsequently.

2.2. Vehicle modelling

In the current study, a 1450 kg base vehicle with 74.5 kW gasoline engine, 5-speed manual transmission, 0.315 m wheel radius and 2.52 m^2 projection area is adopted for the conventional vehicle model. 1.225 kg/m^3 air density, 0.35 drag coefficient and speed-depended rolling resistance coefficient are used for simulations.

The theoretical model of the conventional vehicle is designed by using MATLAB Simulink. The vehicle model consists of parameters, road resistance, transmission, power source (engine) and engine maps sub-models which are also in common with the hybrid vehicle model. Basically, parameters sub-model contains driving cycle speed variations, vehicle and environmental parameters while road resistance sub-model calculates total resistive forces by using those information. In transmission sub-model gear ratio is determined, then transmission efficiency is included in addition to gear ratio to calculate power demand and engine speed by power source sub-model. Afterwards, determined engine speed and power values are inputted to engine maps sub-model to obtain instantaneous fuel consumption and CO_2 emission values.

In order to design parallel hybrid vehicle power-train, transmission is located between differential and electric motor. This pre-transmission configuration is more advantageous when a small electric motor with the same speed region as the engine is used [23]. The layout of parallel hybrid power-train system and electric energy flow of the vehicle is given in Fig. 3.

In the electrical system, a 15-kW electric motor, whose maximum speed is 8000 rpm, is chosen, and its efficiency map is used for hybrid vehicle simulations. Low power electric motor such as 15 kW was selected since the parallel hybrid powertrain configuration was adopted with high internal combustion engine power. It is aimed to use the motor in order to meet low power demands, which leads engine to be at rest during these inefficient operation conditions for the ICE. While the choice of electric motor power, the two main concerns were to meet high amount of in-city condition with low-power demands and to transfer ICE operations to regions which have high power and hence efficiency, but have reasonable speed range nevertheless. In other words, maximum EM power sets the lower limit of ICE operations and it is determined so high as to ensure adequately low BSFC of ICE operations and so low as to keep the ICE operation range wide and to keep electrical system weights low. Therefore, 15-kW EM is adopted to 75-kW ICE and hence widely used EM power and ICE power ratio is obtained [7,12,13,14,19,24]. Some power ratios of EM and ICE, which are used in similar hybrid configurations from the literature, can be seen in Table 2. In order to supply energy for the electric motor, a battery is adopted, which has 2.5 kWh energy capacity.

Efficiency values of the components in the electrical part of the powertrain such as battery, motor and converter are considered as maps in the study. Hence, efficiency maps of the mentioned components are simulated as 2D look-up tables in the Simulink model. Efficiency values are altered depending on the change of power and SoC for battery, torque and speed for electric motor including converter. While doing so, transmission efficiency is assumed to be constant during simulations.

At the beginning of simulations, SoC of battery values are set as to obtain equal initial and final battery SoC, which is called as charge-neutral simulation [25], in order to avoid extra energy consumption for electricity accumulation or mechanical energy gain by battery discharge. This led the conventional and hybrid simulations to be compared without calculating gasoline equivalent electrical energy since the engine and the electrical system efficiency is varying instantaneously during charge (generator) or discharge (motor) operations.

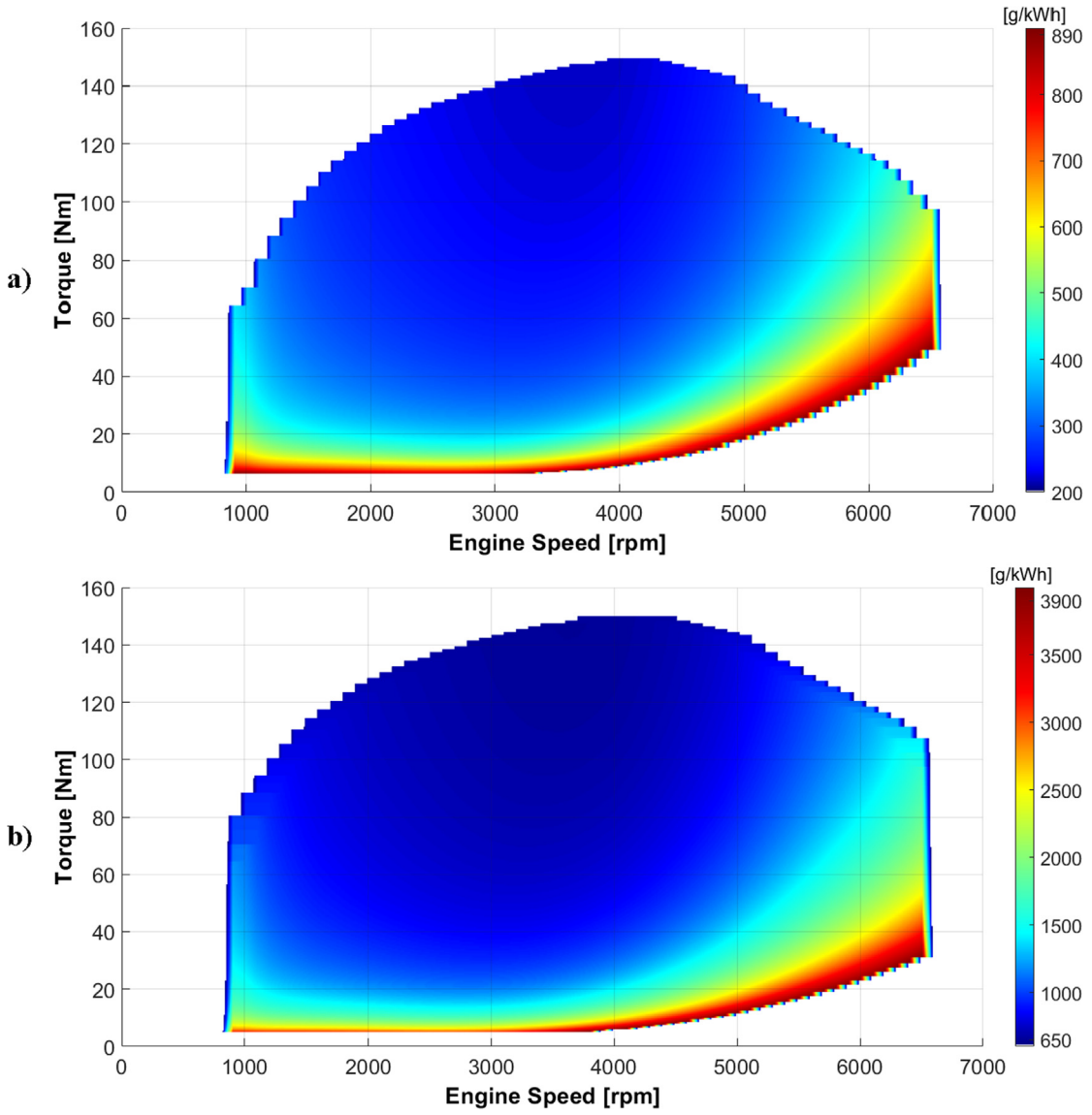


Fig. 2 a) 2D descriptions of brake specific fuel consumption and b) CO_2 emission values depending on torque and engine speed.

Overall electrical system efficiency during simulations are calculated as comparable quantities of hybrid vehicle simulations over WLTC and the local route. Overall efficiencies of simulations are obtained by using cumulative energy that given to generator operations and cumulative energy that taken from motor operations which is transmitted through the battery. Namely, it is the ratio of total energy output and input of the electrical system from the ICE to the transmission. Fig. 3b depicts the paths that electric energy flows through.

The theoretical model of the parallel hybrid vehicle is designed by using MATLAB Simulink software. Different sub-models are used in order to build the general Simulink model. Fuel consumption and CO_2 emission values over WLTC and a local driving route, speed data of which are collected in Istanbul city, are obtained by this Simulink model.

Simulink sub-models and general model of the vehicle are shown in Fig. 4. In the hybrid vehicle model, road resistance and gear ratio are obtained as same in the conventional vehicle model. Similarly, total power demand and speeds of power sources are determined in power source sub-model. Powertrain controller decides distribution of total power demand to the engine and the electric motor in accordance with driving mode decision considering SoC of the battery and charging processes. In electrical system sub-model, charge/discharge levels and SoC of the battery are calculated by taking electric motor power, speed and electrical component efficiencies into consideration. Finally, the fuel consumption and emission values are calculated by engine maps sub-model resulted from ICE power and speed.

2.2.1. Hybrid vehicle algorithm

Fig. 5 depicts the demonstration of various engine operating zones and the powertrain control algorithm of hybrid vehicle, where EM_{max} and ICE_{max} are maximum power values of the electric motor and the internal combustion engine, respectively. EM_{min}, which is a negative value, is the maximum power of the electric motor during generator mode. P_{dem} is instantaneous power demand by the vehicle from powertrain, which

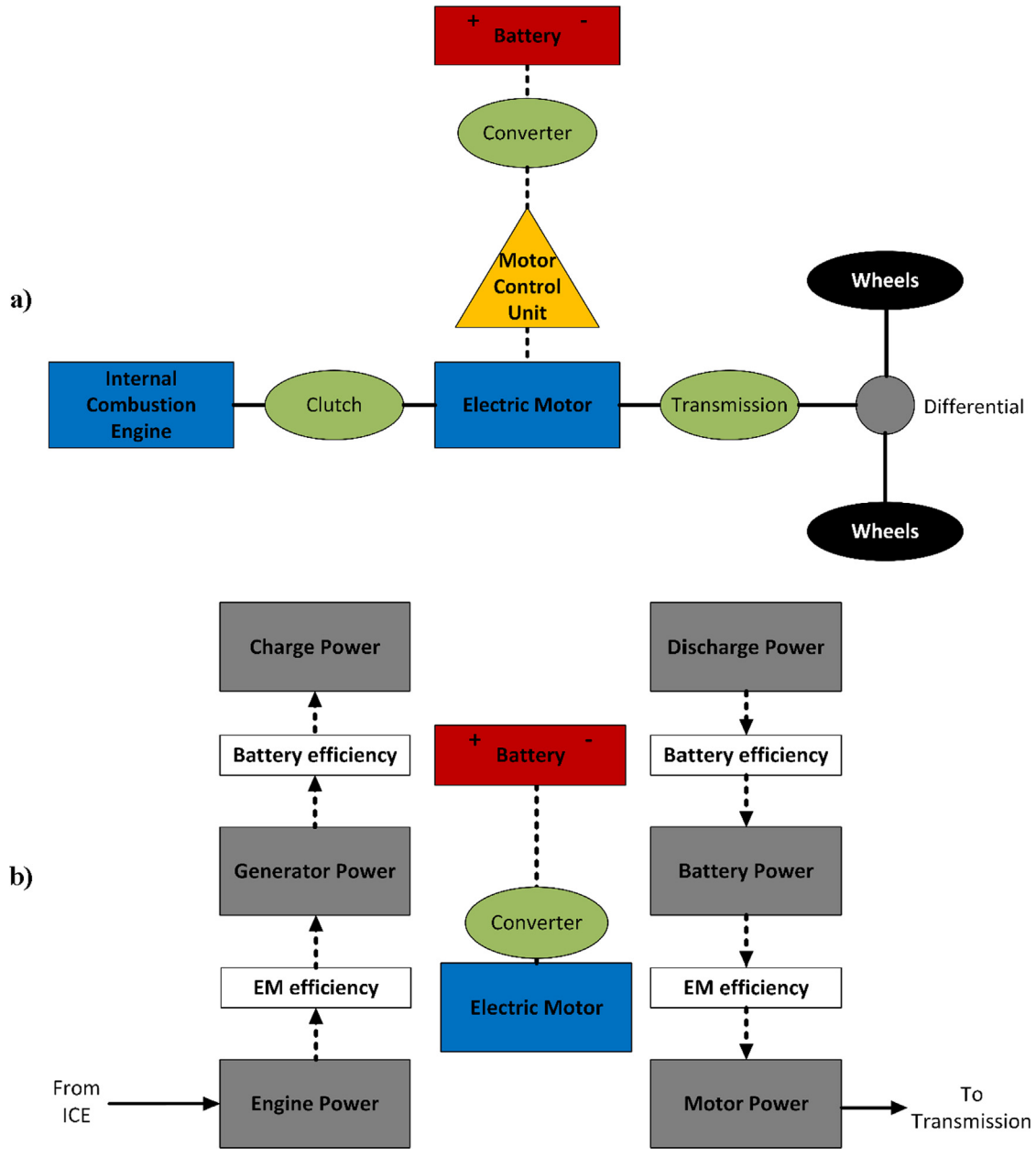


Fig. 3 a) Powertrain schematic and b) paths of electric energy flow of parallel hybrid vehicle.

meets road resistances (rolling, aerodynamic, slope) and ensures instantaneous acceleration of the cycle. The variable n_{ICE} is instantaneous engine speed, n_{lower} and n_{upper} are the determined limits of engine speed with which the engine operates with low BSFC. SoC_{lower} is the determined state of charge lower limit of efficient region of the battery, which should not be decreased. SoC_{upper} is the target SoC value in the case of reaching the SoC_{lower} limit. $SoC_{highest}$ is the determined SoC higher limit of efficient region of the battery, which should not be exceeded and is very close to 100%. The variable $ratio_{eff}$ is value depending on the current engine speed in order to determine the power values range of low BSFC region of the engine between n_{lower} and n_{upper}. In other words, low BSFC region was between $ICE_{max} \cdot ratio_{eff}$ and ICE_{max} and it was calculated for current engine speed at each simulation step. P_{ICE} and P_{EM} are the instant power values of the ICE and the electric motor, respectively, distributed by the control units of the ICE and the motor. In the algorithm, $charge = 1$ implies that the electric motor generates power for the battery.

In Fig. 5b, A, B and C parts of the algorithm correspond to relevant regions in the Fig. 5a. While P_{dem} is in region A, electric motor power is enough and ICE operation is not required (Case 3). However, if P_{dem} - EM_{min} is in efficient region of the ICE and if SoC is lower than $SoC_{highest}$, then the electric motor operates as generator and road resistances and power generation of the electric motor with partial or maximum generator power are met by ICE operations in its low BSFC region (Case 1 and 2). If SoC of the battery happens to drop below the crit-

Table 2 Similar EM/ICE power ratios of parallel hybrid vehicles in the literature.

Reference	ICE Power	EM Power	Unit	EM/ICE Power Ratio
[2]	100	30	kW	0.30
[7]	165	44	kW	0.27
[12]	100	41	HP	0.41
	100	24	HP	0.24
	105	41	HP	0.39
	105	24	HP	0.23
[13]	110	25	kW	0.23
[14]	210	30	kW	0.14
[19]	73	15	kW	0.21
[24]	188	40	kW	0.21
	188	45	kW	0.24
[26]	96	32	kW	0.33

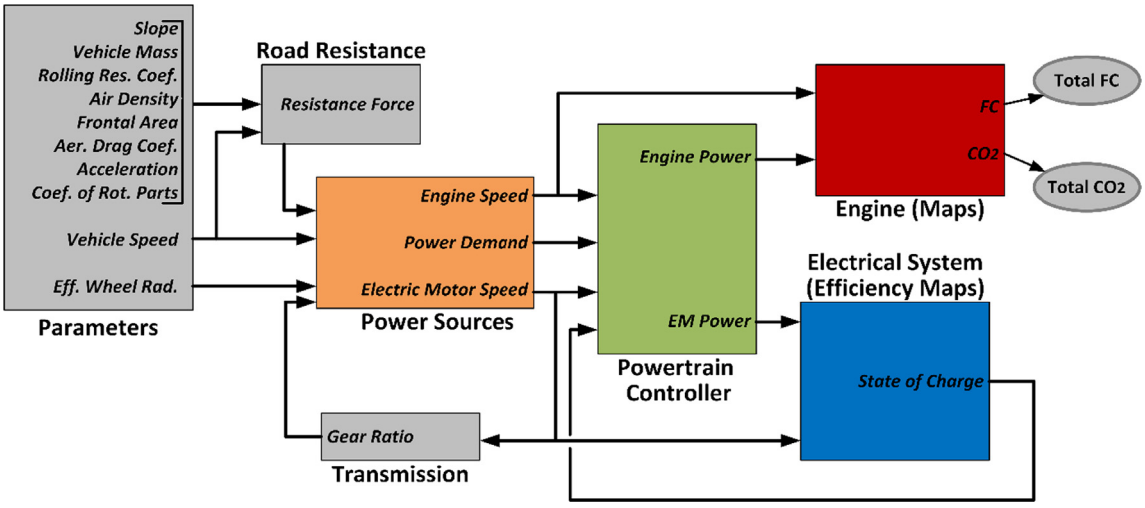


Fig. 4 Model of the hybrid vehicle.

ical value (SoC_{lower}), the ICE operates to charge the battery until it reaches SoC_{upper}, which is determined in order to create hysteresis and to avoid undesired consecutive generator on–off operations (Case 4). While P_{dem} is in region B, if SoC is above the higher limit of battery efficient region ($SoC_{highest}$), ICE meets only P_{dem} and battery is not charged (Case 5). Otherwise, the ICE charges the battery with partial or maximum generator power and therefore produces more power and operates in its lower BSFC regions (Case 6 and 7). While P_{dem} is in region C, the ICE and the electric motor operate simultaneously to meet P_{dem} and therefore battery charging is not possible (Case 8).

In brief, the hybrid algorithm does not let the engine to operate under 15 kW power demand regions (Cases 1–4 in Fig. 5b) except to charge the battery when SoC drops down below the allowed lower bound during low engine speeds. Moreover, charging processes also tends to be realized by the algorithm during higher power demand than maximum motor power (15 kW). This behavior tends to transfer high amount of operation duration to regions over 30 kW power.

2.3. Overall model schematic

In this study, the engine data of the reference vehicle is obtained by using common OBD instruments over CANBUS vehicle communication protocol. Then, fuel consumption and CO_2 emission maps are generated by using artificial neural network. Afterwards, the parallel hybrid vehicle design and the algorithm are developed for which the generated maps are used as inputs. Finally, with developed vehicle model, instantaneous fuel consumption and CO_2 emission values are obtained in WLTC and through the local driving route. The general schema of data acquisition and simulations is given in Fig. 6.

3. Results and discussion

As mentioned before, the brake-specific fuel consumption, the CO_2 maps and the local driving route speed variation are created by using the vehicle data obtained. Then, conventional and hybrid vehicle models are built in Matlab/Simulink

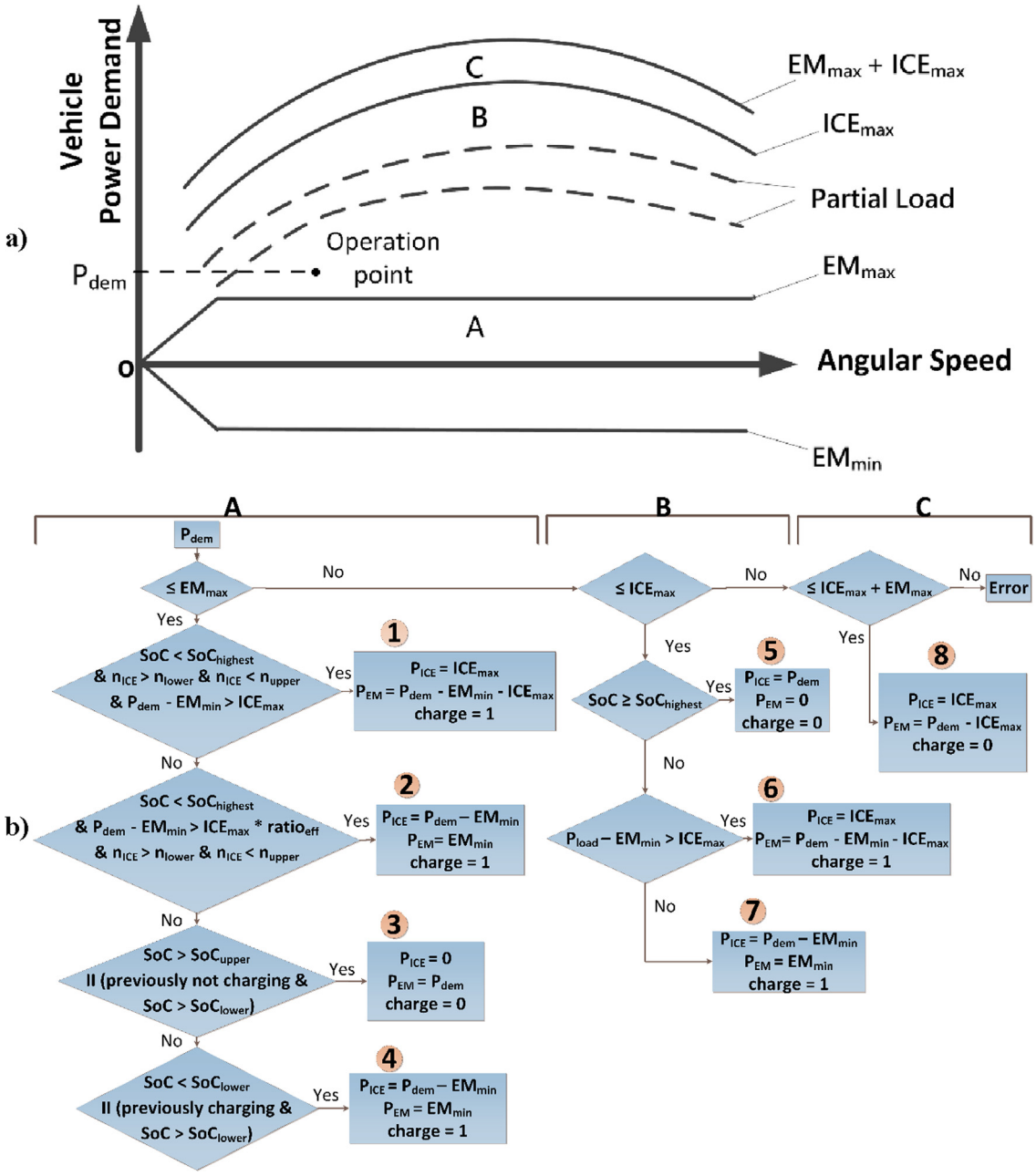


Fig. 5 Demonstration of a) various operating zones and b) algorithm of hybrid vehicle control respectively.

software by adding the control algorithm, electric motor and battery efficiency maps. Afterwards, the simulation results obtained from WLTC and the local driving route are compared.

3.1. Driving cycles

The speed, acceleration and the power requirement variations of modelled vehicle during WLTC and the local driving route are shown in Fig. 7.

As mentioned before, EM power is chosen to meet operation durations of low-power demand, in-city conditions which are mostly located in the first 500 s for both cycle. During WLTC and the local route, 73.7% and 84.0% of positive power demand durations require below 15 kW, respectively.

In Table 3, some fundamental values of WLTC and the local route used in this study are given briefly.

As can be seen in Fig. 7 and Table 3, for a conventional vehicle with ICE, the local driving route is more disadvantageous in terms of BSFC, due to its lower power and speed requirement variations.

3.2. Power consumptions

The ICE and the electric motor power variations of conventional vehicle and hybrid vehicle can be seen in Fig. 8. Some

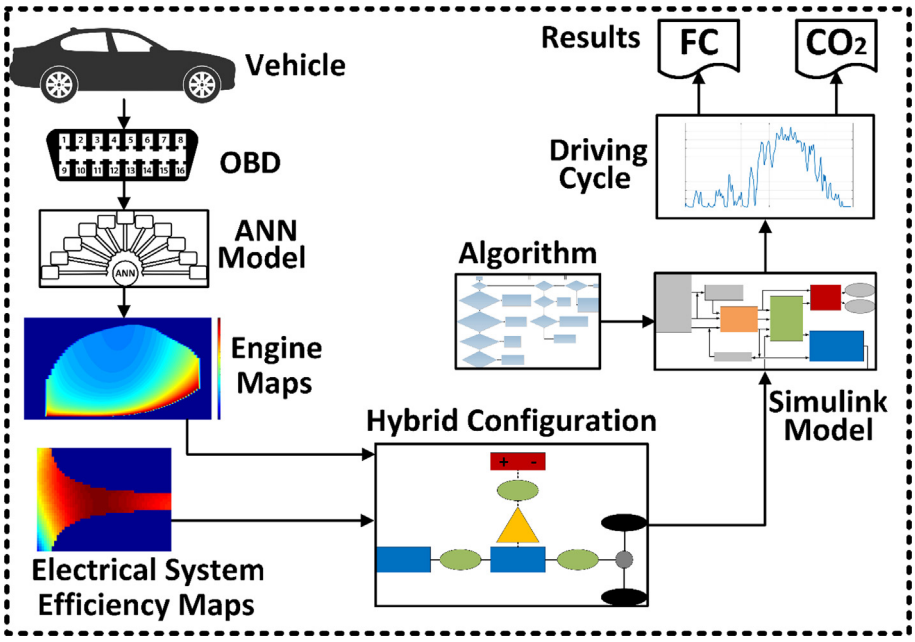


Fig. 6 Schema of overall experimental and theoretical processes.

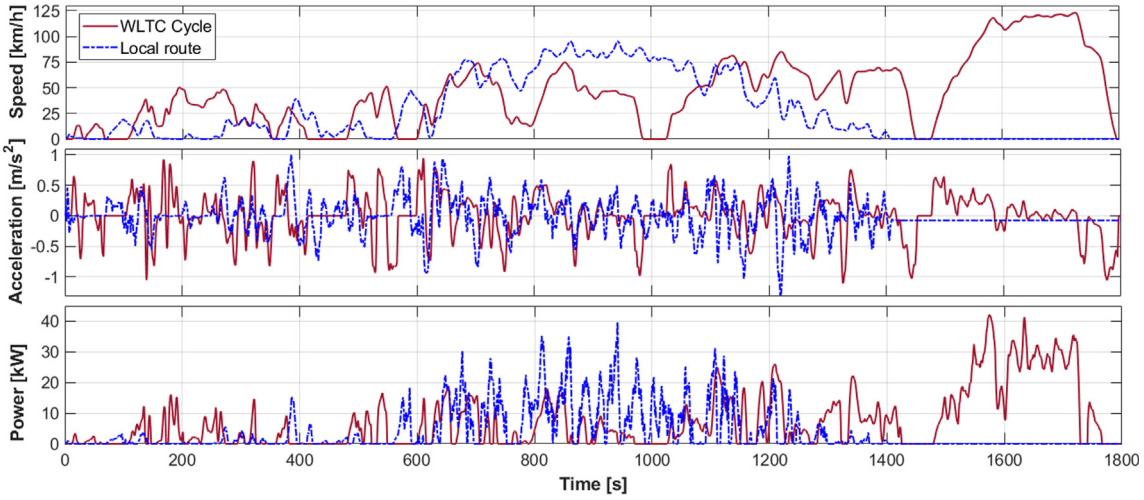


Fig. 7 Speed, acceleration and power requirement variations during WLTC and the local driving route, respectively.

regions of the graphs are selected to zoom, which are given in Fig. 8b and Fig. 8d, and to make brief explanations.

As can be noticed, during the generator operations of electric motor (negative values), the ICE of the hybrid vehicle produces more power than the ICE of the conventional vehicle, while the electric motor sometimes operates on its own. Moreover, while electric motor is not operating as generator, power of the hybrid vehicle is slightly higher than that of conventional vehicle due to additional weights such as battery, electric motor and convertor. Mentioned difference is more apparent while acceleration durations (e.g. 1290–1309 s in Fig. 8b) in which vehicle mass is more dominant parameter.

In the first part of Fig. 8b, until 1283 s, low power requirement occurs, which is supplied by the electric motor only (Case 3). Later (1283–1290 s), power demand is still in the range of the EM but engine operation with charging the battery is decided to be efficient and therefore the hybrid ICE meets road resistance and charges the battery (which expressed as negative EM values) by producing higher power than that of the conventional ICE. Charging is realized with partial generator

Table 3 Details of the cycles.

Driving Cycle	WLTC Class 2	Local driving route
Distance [km]	22.649	13.684
Total time [s]	1800	1481
Idle time [s]	240	198
Average speed [km/h]	45.3	33.6
Average driving speed [km/h]	52.3	38.4
Maximum speed [km/h]	123.1	95.4
Maximum acceleration [m/s^2]	0.96	1.02

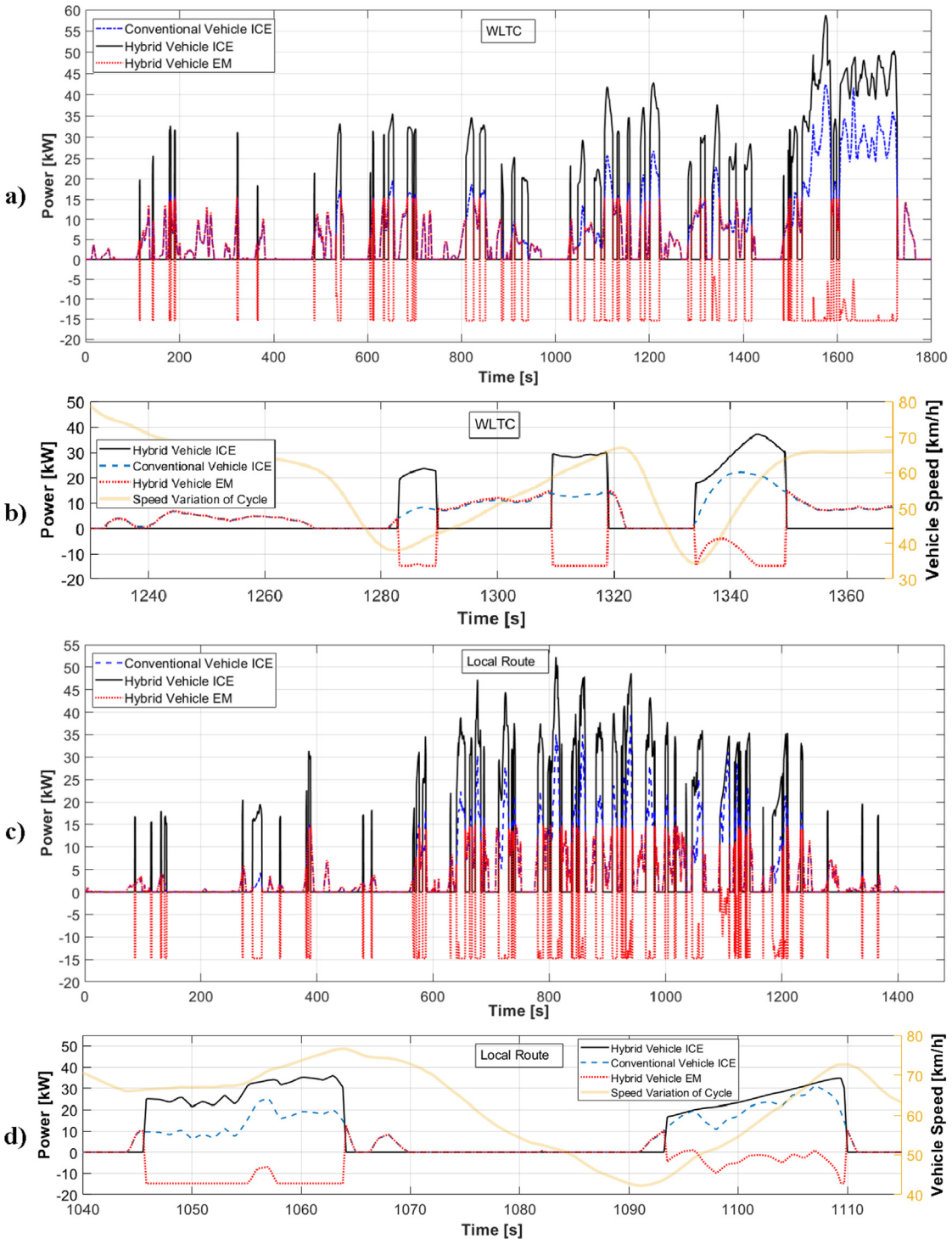


Fig. 8 Power variations of conventional vehicle ICE, hybrid vehicle ICE and electric motor a) during WLTC and b) its zoomed in view, c) during the local driving route and d) its zoomed in view.

power between 1285 and 1287 s (Case 1) while the battery is being charged with maximum generator power during the rest (Case 2). Then (1290–1309 s), the engine quits its efficient region and the EM is involved to meet low road resistances while the ICE is at rest (Case 3). Afterwards (1309–1319 s), power demand is still in the range of the EM but the battery charge is dropped down below allowed lower limit and therefore the ICE charges the battery up to determined SoC value (Case 4). Then, it is followed by EM operation for low power demand (1319–1322 s) (Case 3). After vehicle coast down or braking with no power demand (1322–1334 s), sudden vehicle speed increase duration requires high power. This requirement is met by the ICE and remaining power of the ICE charges the battery with partial generator power (1334–1344 s) (Case 6). In

the following duration (1344–1350 s), ICE power is sufficient to meet both road resistance and battery charge with maximum generator power (Case 7). Afterwards, low power demand is met by EM only (Case 3). Differently from WLTC sample region, power demand slightly exceeds the sum of ICE and EM maximum power for a short while (1095–1096 s) of local route sample region in Fig. 8d. This high power requirement is met by initiation of both the ICE with its maximum power and the EM with its partial power (Case 8).

During the simulations, hybrid vehicle efficiency variations of the electric motor and the battery are shown in Fig. 9.

At the beginning of simulations, SoC of the battery values are assumed to be at the efficient region of the battery (above SoC_{lower}) in order to ensure comparable efficiency conditions during both cycles.

According to hybrid vehicle simulation results, the total amount of energy flow through the battery is 1.51 kWh and 0.90 kWh for WLTC and the local route, respectively. Although the flow of energy value of the local route is lower, its percentage value is higher, since total energy requirements of the hybrid vehicle during WLTC and the local route are 3.60 kWh and 1.95 kWh, respectively. This shows that the local route leads electrical system to supply larger proportion of total energy requirement. In other words, the benefit of a hybrid vehicle becomes more prominent for the city driving conditions. On the other side, a slight difference exists between the overall efficiency values of the electrical system during WLTC and the local route, which are 65.88% and 63.37%, respectively. This difference can be explained by electric motor operations at very low speeds which are low efficient for the electric motor. This type of operations are more frequent in the local driving route.

3.3. Fuel consumptions

Fig. 10 depicts the ICE operating points of the conventional and the hybrid vehicles during WLTC and the local driving route in terms of the brake-specific fuel consumption.

In both conventional and hybrid vehicle simulations, engines are practically used in the speed range between idle speed and 4000 rpm. Since the maximum speeds of the ICE and the EM are close to each other, the base vehicle transmission is used for hybrid vehicle as well. Gear ratios of the 5-speed transmission and the differential are 3.583, 1.926, 1.281, 0.951, 0.756 and 4.250, respectively.

For both driving cycles, internal combustion engine operating points of hybrid vehicle were transferred to higher torque values, which produce lower break specific fuel consumption values. The flexibility for an ICE to operate more efficient zones has more noticeable effects on BSFC values under the city driving conditions, since the local route power and speed requirements are lower than those of the WLTC cycle and hybrid system eliminates these low-efficient zone operations [13].

In order to provide better presentation of engine operations in torque–speed plane, color maps are created and given in Fig. 11. In the maps, distribution of total operation durations of conventional vehicle engine (Fig. 11a and b) and energy generations by the engines of conventional and hybrid vehicles over WLTC (Fig. 11c and e) and the local route (Fig. 11d and f) can be seen in discretized small regions of torque–speed plane. Engine energy generations are calculated by engine speed, engine torque and operation durations for each step of simulations. Although idling has less effect on fuel consumption, idle operations without torque production, which are concentrated on one particular small region, have long total duration compared to other regions. Therefore, those operations, whose durations are 240 and 198 s for WLTC and the local route, are not included in the duration color maps (Fig. 11a and b) to obtain sufficient contrast between regions.

It is obtained that the ICE of the base vehicle operates at low-efficient regions which fall below 15-kW curve, during 1495.8 and 1302.3 s over 1800-second WLTC and 1481-second local route, respectively. In addition, it is calculated that mentioned low-efficient operations were responsible for 1537.8 Wh and 912.6 Wh energy generations by the conventional vehicle engine over WLTC and the local route, respectively. These energy values, which have direct effect on fuel consumption and CO_2 emissions, are equal to 42.6% and 46.8% of total energy generations of ICE over WLTC (3612.8 Wh) and the local route (1951.8 Wh) simulations with

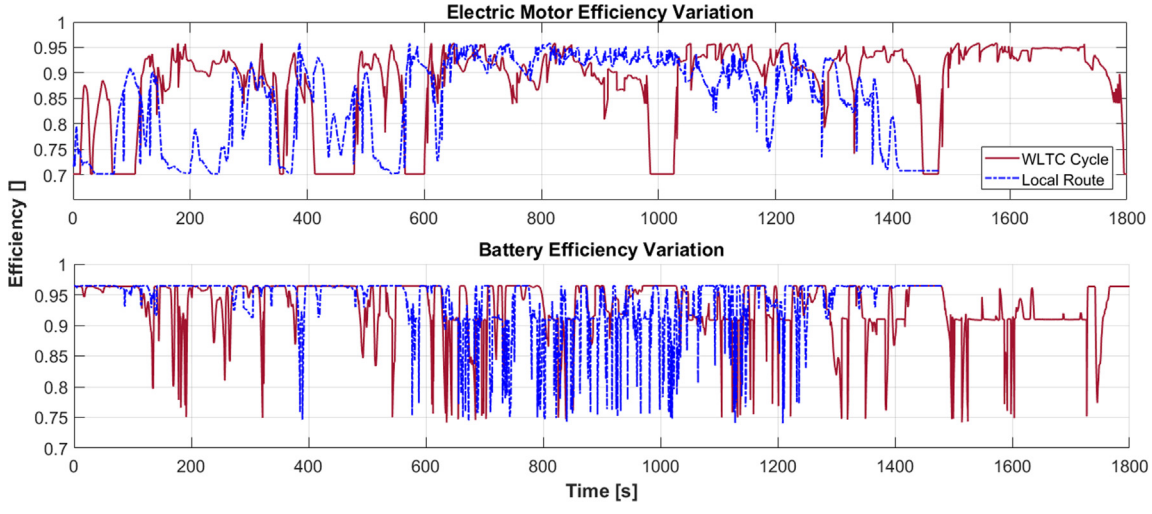


Fig. 9 Efficiency variations of electric motor and battery during WLTC and the local driving route.

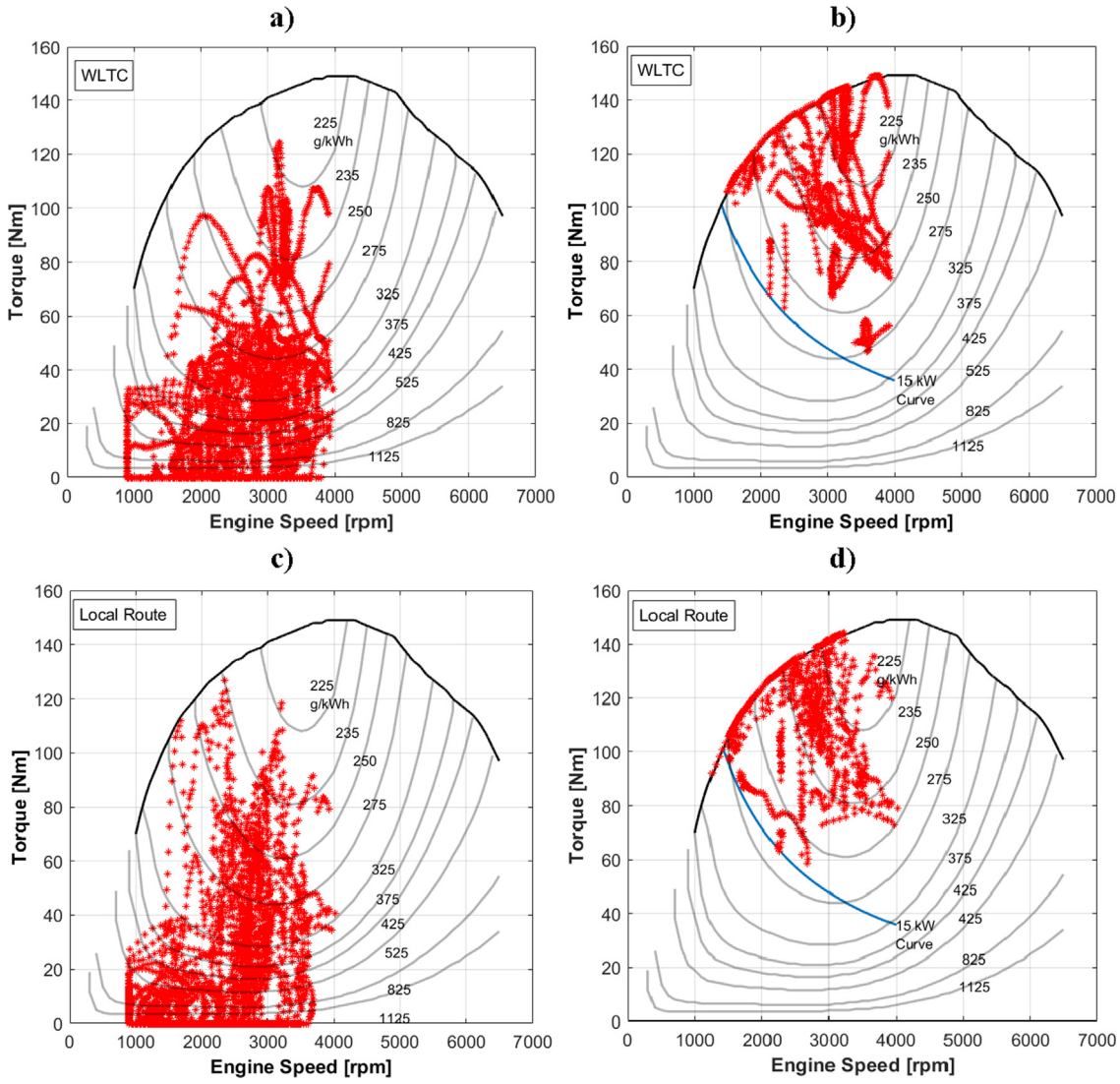


Fig. 10 ICE operation points from simulations in FC maps during a) WLTC with conventional vehicle, b) WLTC with hybrid vehicle, c) the local driving route with conventional vehicle and d) the local driving route with hybrid vehicle.

conventional vehicle, respectively. As stated previously, hybrid vehicle ICE mostly operates over 15 kW power demand, which is significantly more efficient. Moreover, as mentioned before, realizing charge processes, while power demand is over 15 kW, transfers high amount of operation duration and energy generation to slightly more efficient regions over 30 kW power in the engine map. This tendency can be noticed from Fig. 11e and f. ICE operations above 15 kW and 30 kW ensure BSFC values below 325 g/kWh and 250 g/kWh up to 4000 rpm (range that is used in this study) engine speed, respectively. The ICE in this study can provide 15 kW and 30 kW over 1410 rpm and 2220 rpm engine speeds, respectively. Therefore, the ICE operations are mostly limited above 15 kW power in speed range of 1410 rpm and 4000 rpm with 325 g/kWh or less fuel consumption by the choice of 15-kW electric motor.

Local route, operation durations and energy generations of the conventional vehicle engine (Fig. 11b and d) are concentrated in lower power regions than that of WLTC cycle (Fig. 11a and c). Therefore, the use of hybrid powertrain transfers higher amount of duration and energy generation of local route simulations (Fig. 11f) to more efficient regions than that of WLTC simulations (Fig. 11e). By using hybrid powertrain, cumulative energy generation values by engine operations over 30 kW power are increased from 18.6% and 6.3% to 81.2% and 74.7% during WLTC and the local route, respectively. Energy generation distributions in mentioned regions are summarized in Table 4.

Fig. 12 shows the instantaneous fuel consumption variations of the conventional and the hybrid vehicles, and speed values of cycles. Fig. 12b and Fig. 12d show selected parts to present some brief details of WLTC and the local route, respectively.

As expected, some regions of the hybrid vehicle fuel consumption variations have obviously higher values in comparison to the conventional vehicle due to the generator operation of electric motor, while in some regions, the ICE is at rest and fuel consumption is zero during the electric-motor-only operations.

As pointed out in power consumption section, the hybrid vehicle ICE often generates higher amount of power and

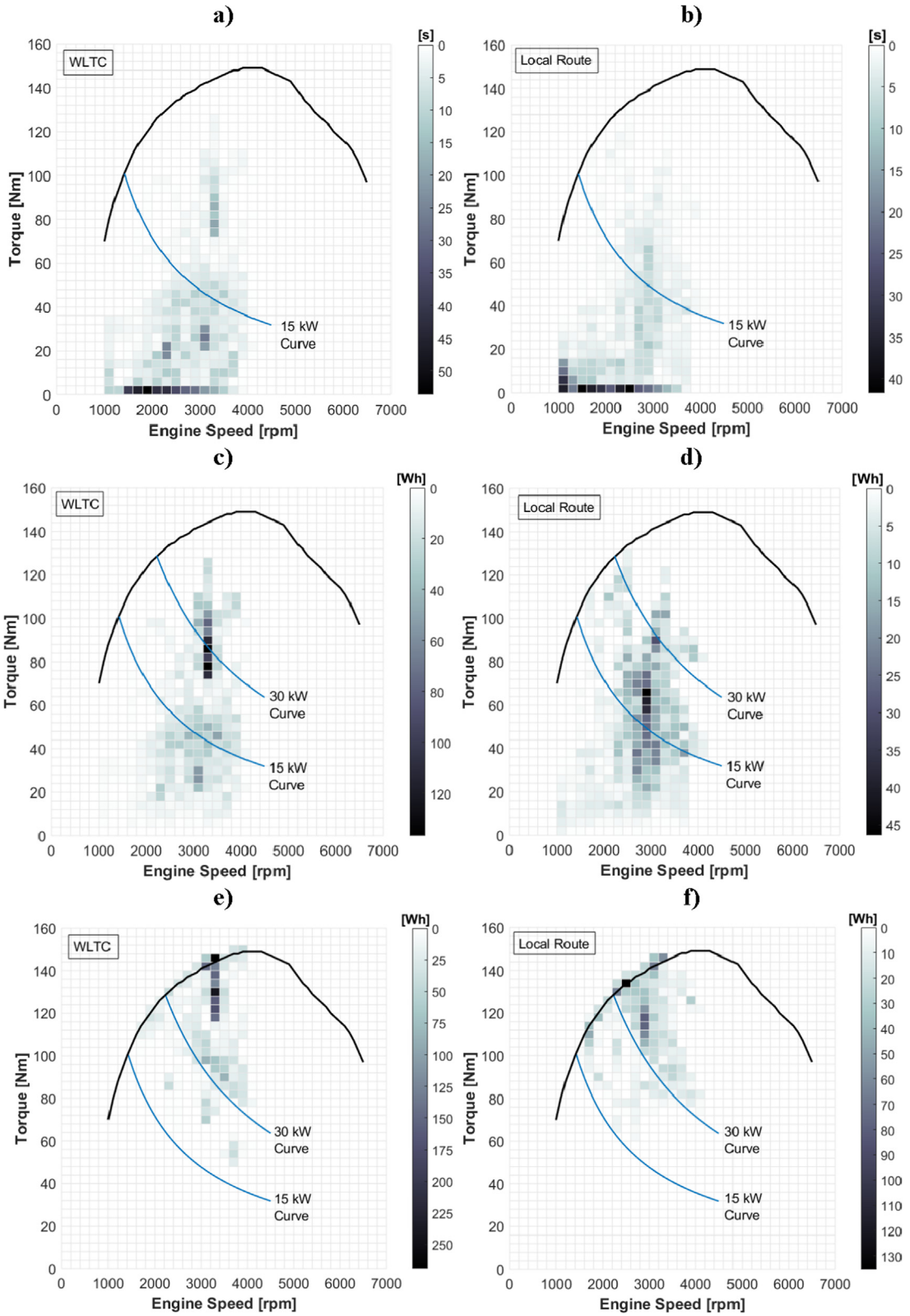


Fig. 11 Distribution of conventional vehicle ICE operation durations during a) WLTC and b) the local route, conventional vehicle ICE energy generations during c) WLTC and d) the local route, hybrid vehicle ICE energy generations during e) WLTC and f) the local route.

hence consumes higher amount of fuel than that of conventional vehicle during high power demand (over 15 kW) and charging operations. However, in most of low power demand durations and idle operations, the ICE is at rest and fuel consumption of the hybrid vehicle is zero as can be seen in Fig. 12b and d.

Table 4 Energy generation distributions of conventional and hybrid engine operations during WLTC and the local route.

		Generated energy by ICE [Wh (%)]			
		0–15 kW	15–30 kW	> 30 kW	Total
WLTC	**Conv. vehicle**	1537.8 (42.6)	1401.3 (38.8)	673.8 (18.6)	3612.8
	Hybrid vehicle	0.0 (0.0)	827.5 (18.8)	3565.3 (81.2)	4392.9
Local	**Conv. vehicle**	912.6 (46.8)	916.1 (46.9)	123.1 (6.3)	1951.8
	Hybrid vehicle	3.3 (0.1)	619.3 (25.2)	1832.4 (74.7)	2455.0

As a result of the simulations, the total fuel consumption values of the conventional and the hybrid vehicles during WLTC and the local route are obtained. The total fuel consumption values are shown in Fig. 13 in terms of L/100 km.

The total fuel consumptions of the conventional and the hybrid vehicles during the WLTC cycle are 6.97 L/100 km and 6.01 L/100 km, respectively. In the local route, 7.01 L/100 km and 5.64 L/100 km consumption results are obtained for the conventional and the hybrid vehicles. The fuel consumption reductions for WLTC and for the local route are 13.77% and 19.54%, respectively.

As mentioned before, the hybrid system provides more efficient ICE operations in terms of BSFC, and therefore reduces the total fuel consumption. Moreover, the benefit of hybrid vehicle becomes more prominent due to higher electric motor usage rate and provide more fuel consumption reduction under the city driving conditions. Additionally, the hybrid system eliminates more low-efficient ICE operations under city driving conditions in compared to the WLTC cycle. From this point of view, it can be said that the hybrid vehicles are advantageous especially in low speeds with high acceleration values and continuously variable acceleration motion regime in terms of the fuel consumption. Lujan et al [26] compared WLTC and real driving condition, and showed that hybrid vehicles would give better results than conventional vehicles with the increase of variable speed conditions and acceleration value. Based on this, the results show a parallel trend with Lujan et al. [26].

3.4. CO_2 emissions

Carbon dioxide is a non-toxic ingredient of the atmosphere, however high concentration of CO_2 has harmful effects on climate due to its greenhouse effect [27].

Although emission values, such as NO_X THC and CO are affected by operation conditions of the ICE and combustion characteristics, CO_2 emission value is substantially dominated by fuel consumption value. [28] In other words, fuel consumption has a dominant effect on CO_2 emission, since conversion of all C content of fuel into CO_2 is one of the main targets to increase efficiency and reduce harmful emissions [29]. Therefore, the most effective way to reduce CO_2 emission is to reduce fuel consumption [30].

Fig. 14 depicts the ICE operating points of conventional and hybrid vehicle during WLTC and the local driving route in CO_2 emission maps.

The ICE operation points are transferred to more advantageous zones in terms of CO_2 emission as in fuel consumption results.

The instantaneous CO_2 emission variations of the conventional and the hybrid vehicles as well as the speed values of WLTC and the local route can be seen in Fig. 15.

Similarly to those of fuel consumption variations, CO_2 emissions of the hybrid vehicle are concentrated mostly in high power requirement regions and charging operations. On the other hand, the hybrid vehicle ICE is at rest, and hence it emits zero emission, during the EM is propelling the vehicle or idling operations in contrast with the conventional vehicle ICE.

Both of the WLTC cycle and the local route simulation results of CO_2 emissions for the conventional and the hybrid vehicles are presented in Fig. 16.

Since CO_2 emission and fuel consumption values are supposed to have similar characteristics, hybrid vehicle ICE was operating in the advantageous regions in terms of CO_2 emissions in comparison to conventional vehicle, due to similar reasons with BSFC values. Hence, during WLTC and the local driving route, lower CO_2 emission values are obtained as a result of the hybrid vehicle simulations.

The CO_2 emission results of the conventional and the hybrid vehicles during the WLTC cycle are 153.9 g/km and 132.6 g/km, respectively. In the local route, 154.9 g/km and 124.5 g/km consumption results are obtained for conventional and hybrid vehicles. According to this observed CO_2 values, a vehicle which emits more CO_2 in the conventional driving mode, may emit lower CO_2 in the hybrid driving mode in comparison to different driving cycles. This shows that the engine's operating speed and load play a significant role in efficiency and thus in CO_2 emissions. These results are supported by the study of Al-Samari [13].

Cumulative fuel consumption and CO_2 emission values of conventional and hybrid vehicles over the WLTC driving cycle and the local driving route are also summarized in Table 5.

4. Conclusion

In this study, 3D engine maps were created by using the data obtained through CanBus protocol with the help of the ANN model. And then, the fuel consumption and CO_2 emission data of the vehicle model developed with Matlab-Simulink and of the exemplary conventional gasoline fueled vehicle as well as the parallel hybrid system were compared. Such data in question were obtained under the working conditions of the WLTC driving cycle and of the selected route.

An on–off control method is used for hybrid powertrain simulations by the developed algorithm. More sophisticated predictive method can be used in order to provide further improvements in terms of fuel consumption and emissions. And the hybrid vehicle model can not be validated by experimental results. The findings of the study are summarized as below:

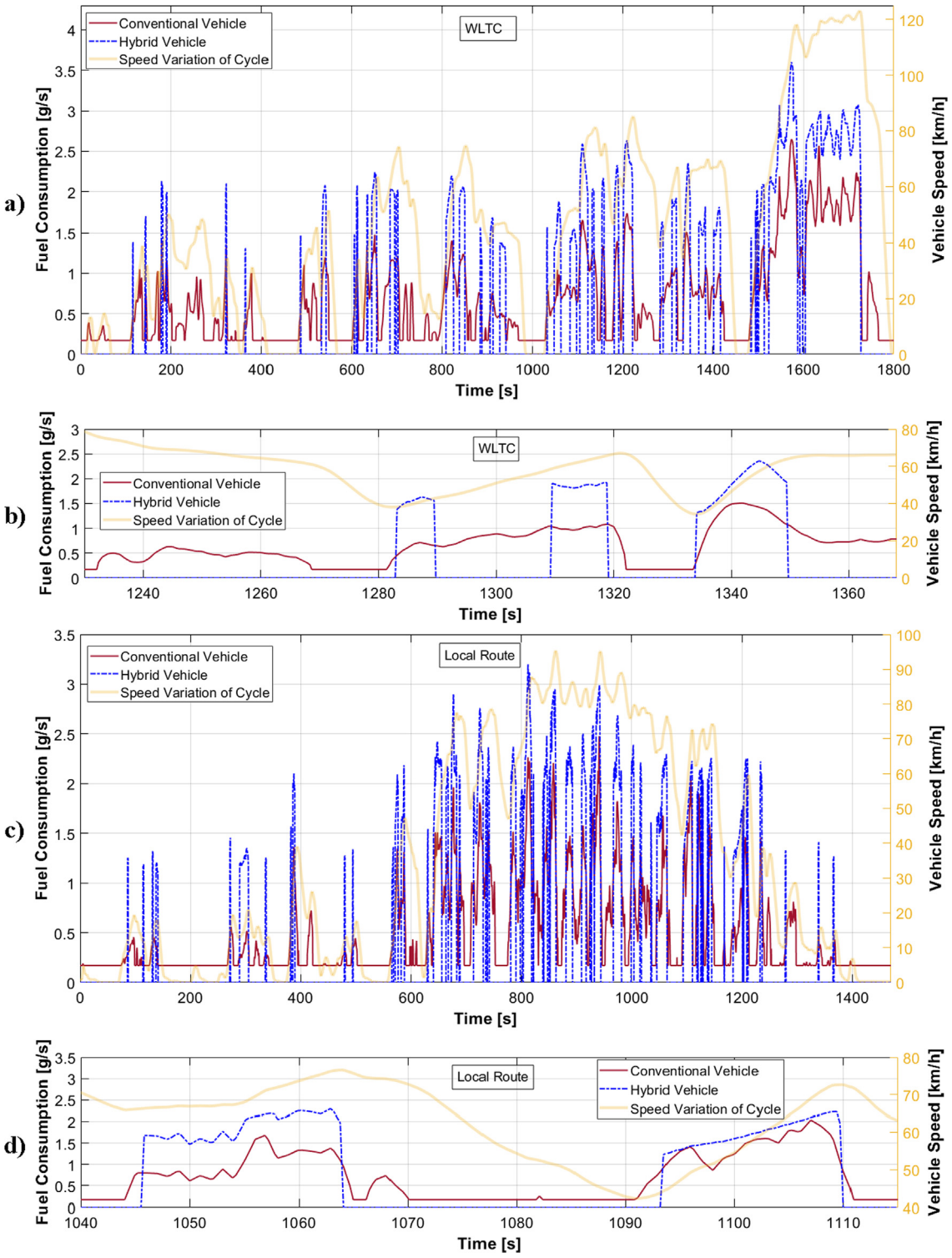


Fig. 12 Fuel consumption variations of conventional and hybrid vehicles a) during WLTC and b) its zoomed in view, c) during the local driving route and d) its zoomed in view.

- Compared to the conventional gasoline fueled vehicle, the fuel consumption values of the parallel hybrid vehicle decrease by 13.77% and 19.54% in the WLTC driving cycle and in the local driving route, respectively.
- While the CO_2 emission release in conventional parallel hybrid driving system decreases from 153.9 g/km to 132.6 g/km in the WLTC driving cycle compared to conventional gasoline fueled engines, in the local driving route, it decreases from 154.9 g/km to 124.5 g/km.

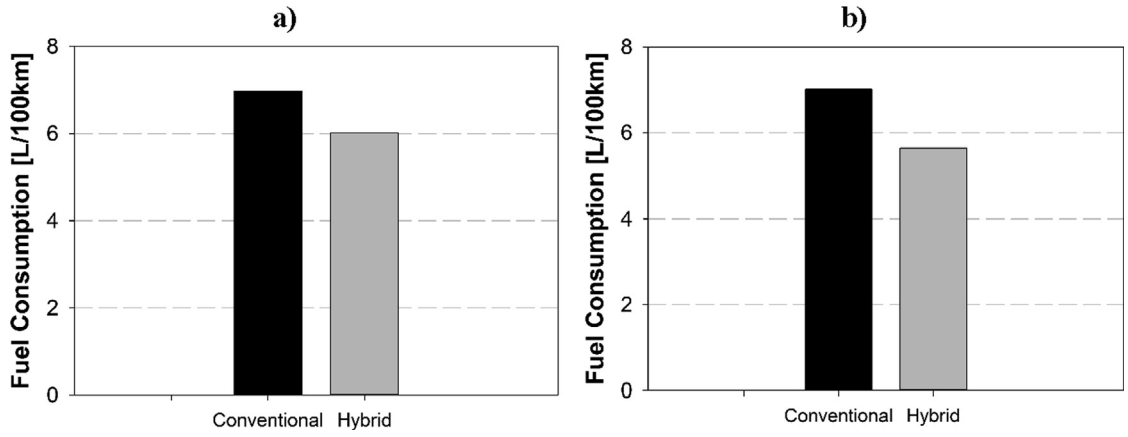


Fig. 13 Cumulative fuel consumption values of the conventional and the hybrid vehicles a) during WLTC and b) the local driving route.

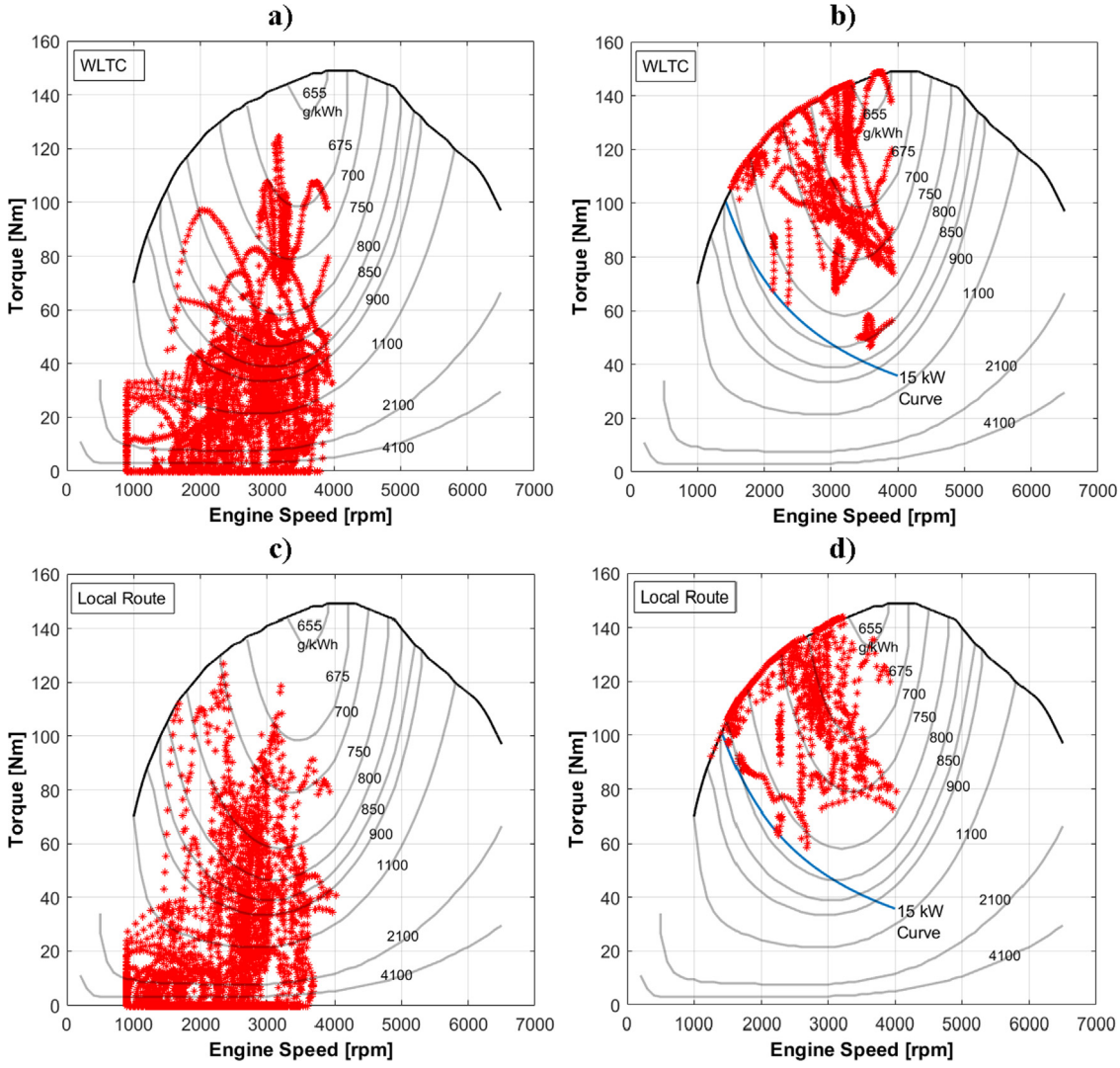


Fig. 14 ICE operation points from simulations in CO_2 maps during a) WLTC with conventional vehicle, b) WLTC with hybrid vehicle, c) the local driving route with conventional vehicle and d) the local driving route with hybrid vehicle.

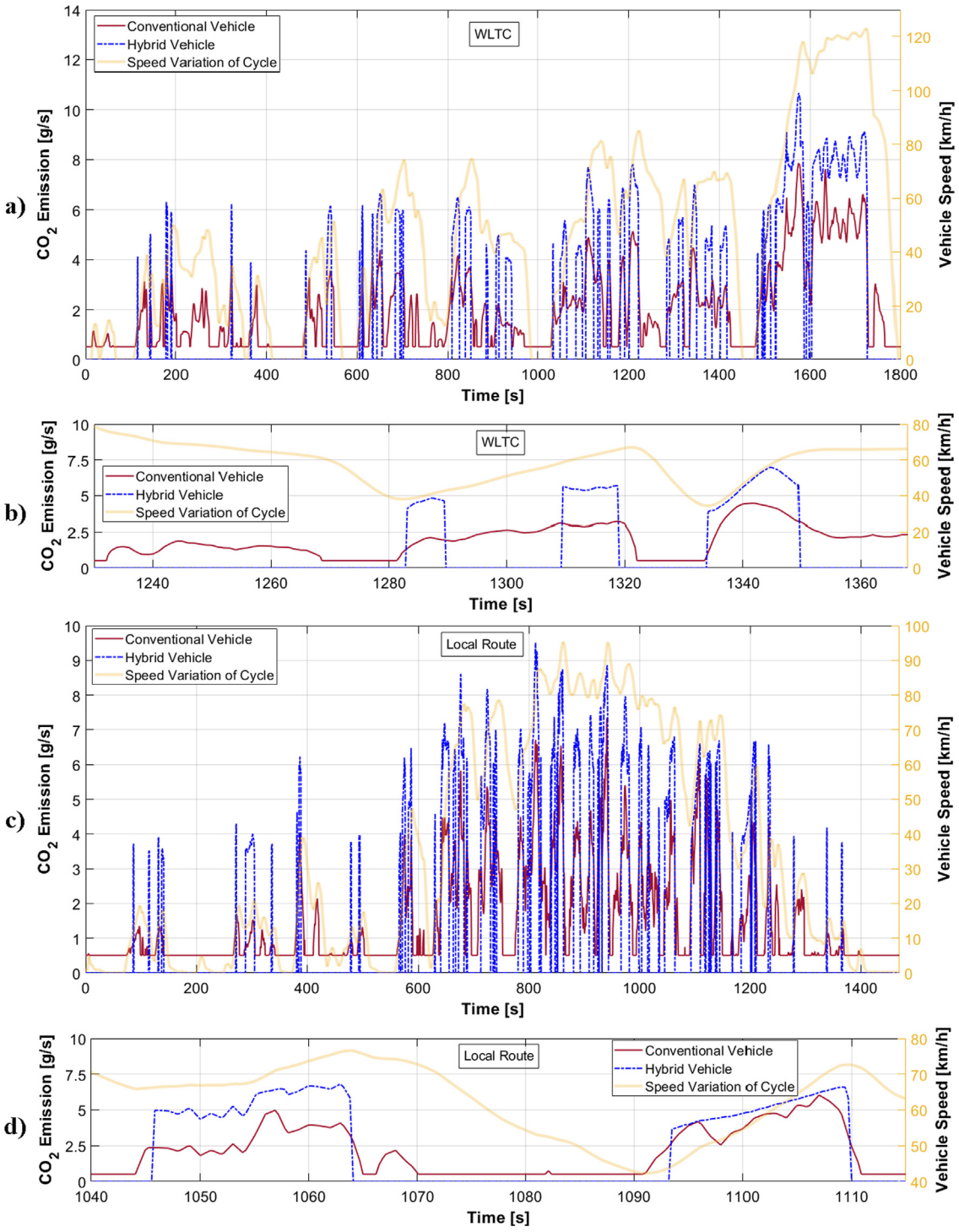


Fig. 15 CO_2 emission variations of conventional and hybrid vehicles a) during WLTC and b) its zoomed in view, c) during the local driving route and d) its zoomed in view.

- During the local route simulation, higher proportion of engine energy generation in inefficient and low power region is transferred to efficient and high power regions by means of hybrid powertrain compared to the WLTC cycle.
- In the current hybrid configuration and algorithm, electric motor mostly propels the vehicle in low power demand. After launch process, very low vehicle speed conditions cause the electric motor to operate with low rpm and low efficiency. High proportion of this type of operations over local route can reduce overall electrical system efficiency while it increases electrical system operation duration.
- In addition, based on the findings, it was concluded that a significant amount of decrease in the fuel consumption and CO_2 emissions was possible to be achieved with an

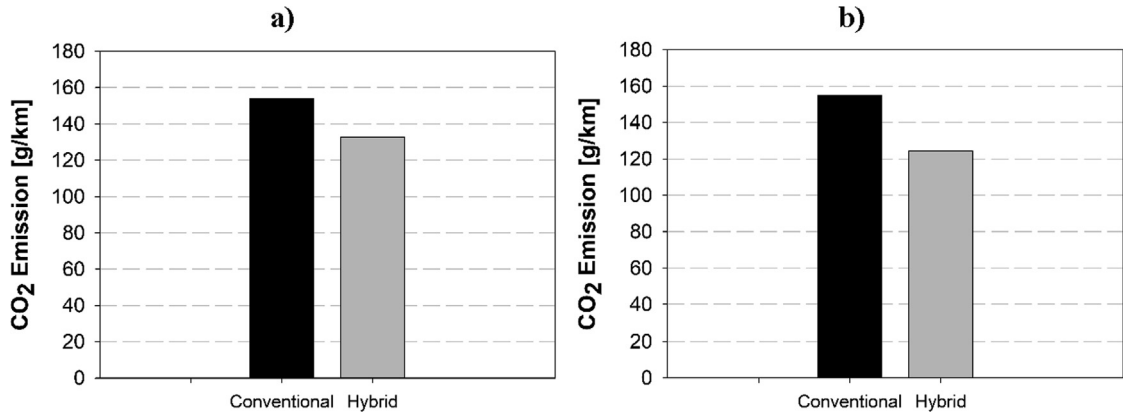


Fig. 16 The cumulative CO_2 emission values of conventional and hybrid vehicles a) during WLTC and b) the local driving route.

Table 5 Summary of cumulative fuel consumption and CO_2 emission values.

	WLTC Class 2		Local driving route	
	Conventional	Hybrid	Conventional	Hybrid
Fuel consumption [L/100 km]	6.97	6,01	7.01	5.64
CO_2 Emission [g/km]	153.9	132.6	154.9	124.5

engine calibration for the positioning of internal combustion engines in the most efficient areas on the map as well as with a power management system. It was also concluded that this improvement could be increased more in partial-load conditions.

Declaration of Competing Interest

The authors declare that they have no known competing financial interests or personal relationships that could have appeared to influence the work reported in this paper.

Acknowledgement

The first author of the manuscript was financially supported by TUBITAK (The Scientific and Technological Research Council of Turkey) 2228-B program.

References

[1] Y. Liu, J. Gao, D. Qin, Y. Zhang, Z. Lei, Rule-corrected energy management strategy for hybrid electric vehicles based on operation-mode prediction, J. Cleaner Prod. 188 (2018) 796–806.
[2] R. Finesso, E. Spessa, M. Venditti, Cost-optimized design of a dual-mode diesel parallel hybrid electric vehicle for several driving missions and market scenarios, Appl. Energy 177 (2016) 366–383.
[3] K.D. Huang, S.C. Tzeng, T.M. Jeng, C.C. Chen, Integration mechanism for a parallel hybrid vehicle system, Appl. Energy 82 (2) (2005) 133–147.
[4] J. Ruan, P.D. Walker, N. Zhang, J. Wu, An investigation of hybrid energy storage system in multi-speed electric vehicle, Energy 140 (2017) 291–306.
[5] W. Enang, C. Bannister, Modelling and control of hybrid electric vehicles (A comprehensive review), Renew. Sustain. Energy Rev. 74 (2017) 1210–1239.
[6] H.T. Ngo, H.S. Yan, Configuration synthesis of parallel hybrid transmissions, Mech. Mach. Theory 97 (2016) 51–71.
[7] J. Guo, Y. Ge, L. Hao, J. Tan, Z. Peng, C. Zhang, Comparison of real-world fuel economy and emissions from parallel hybrid and conventional diesel buses fitted with selective catalytic reduction systems, Appl. Energy 159 (2015) 433–441.
[8] S. Hui, J. Ji-Hai, W. Xin, Torque control strategy for a parallel hydraulic hybrid vehicle, J. Terramech. 46 (6) (2009) 259–265.
[9] Y. Zhang, L. Chu, Z. Fu, N. Xu, C. Guo, X. Zhang, P. Wang, Optimal energy management strategy for parallel plug-in hybrid electric vehicle based on driving behaviour analysis and real time traffic information prediction, Mechatronics 46 (2017) 177–192.
[10] L. Tribioli, G. Bella, Reduction of particulate emissions in diesel hybrid electric vehicles with a PMP-based control strategy, Energy Procedia 148 (2018) 994–1001.
[11] F. Millo, C. Cubito, L. Rolando, E. Pautasso, E. Servetto, Design and development of a hybrid light commercial vehicle, Energy 136 (2017) 90–99.
[12] I. Taymaz, M. Benli, Emissions and fuel economy for a hybrid vehicle, Fuel 115 (2014) 812–817.
[13] A. Al-Samari, Study of emissions and fuel economy for parallel hybrid versus conventional vehicles on real world and standard driving cycles, Alexandria Engineering Journal 56 (4) (2017) 721–726.
[14] H.T. Arat, Simulation of diesel hybrid electric vehicle containing hydrogen enriched CI engine, Int. J. Hydrogen Energy 44 (20) (2019) 10139–10146.
[15] M.U. Karaoğlan, N.S. Kuralay, C.O. Colpan, The effect of gear ratıos on the exhaust emıssıons and fuel consumptıon of a parallel hybrid vehicle powertrain, J. Cleaner Prod. 210 (2019) 1033–1041.
[16] M.E. Hmidi, I. Ben Salem, L. El Amraoui, An efficient method for energy management optimization control: Minimizing fuel consumption for hybrid vehicle applications, Trans. Inst. Meas. Control 42 (1) (2020) 69–80.
[17] A. García, P. Carlucci, J. Monsalve-Serrano, A. Valletta, S. Martínez-Boggio, Energy management strategies comparison for a parallel full hybrid electric vehicle using Reactivity Controlled Compression Ignition combustion, Appl. Energy 272 (2020) 115191.

[18] G. Wu, X. Zhang, Z. Dong, Powertrain architectures of electrified vehicles: Review, classification and comparison, J. Franklin Inst. 352 (2) (2015) 425–448.
[19] Y. Yang, X. Hu, H. Pei, Z. Peng, Comparison of power-split and parallel hybrid powertrain architectures with a single electric machine: Dynamic programming approach, Appl. Energy 168 (2016) 683–690.
[20] Wu, X., Cao, B., Wen, J., & Wang, Z. (2008, June). Application of particle swarm optimization for component sizes in parallel hybrid electric vehicles. In 2008 IEEE Congress on Evolutionary Computation (IEEE World Congress on Computational Intelligence) (pp. 2874-2878). IEEE.
[21] C. Yang, X. Jiao, L. Li, Y. Zhang, L. Zhang, J. Song, Electromechanical coupling driving control for single-shaft parallel hybrid powertrain, Science China Technological Sciences 57 (3) (2014) 541–549.
[22] J. Castresana, G. Gabiña, L. Martin, Z. Uriondo, Comparative performance and emissions assessments of a single-cylinder diesel engine using artificial neural network and thermodynamic simulation, Appl. Therm. Eng. 116343 (2020).
[23] M. Ehsani, Y. Gao, S. Gay, A. Emadi, Modern electric, hybrid electric and fuel cell vehicles: fundamentals, theory and design, CRC Press, 2005.
[24] P.G. Anselma, A. Biswas, G. Belingardi, A. Emadi, Rapid assessment of the fuel economy capability of parallel and series-parallel hybrid electric vehicles, Appl. Energy 275 (2020) 115319.
[25] Johnson, V. H., Wipke, K. B., & Rausen, D. J. (2000). HEV control strategy for real-time optimization of fuel economy and emissions (No. 2000-01-1543). SAE Technical Paper.
[26] J.M. Luján, A. García, J. Monsalve-Serrano, S. Martínez-Boggio, Effectiveness of hybrid powertrains to reduce the fuel consumption and NOx emissions of a Euro 6d-temp diesel engine under real-life driving conditions, Energy Convers. Manage. 199 (2019) 111987.
[27] P. Degobert, Automobiles and Pollution, United States, 1995.
[28] P. Mock, J. German, A. Bandivadekar, I. Riemersma, Discrepancies between type-approval and "real-world" fuel-consumption and CO_2 values. The International Council on Clean, Transportation 13 (2012).
[29] International Energy Agency (IEA) (2009). CO2 Emissions from Fuel Combustion. Paris: International Energy Agency.
[30] Cubito, C. (2017). A policy-oriented vehicle simulation approach for estimating the CO2 emissions from Hybrid Light Duty Vehicles (Doctoral dissertation, Ph. D. Thesis, Politecnico di Torino, Torino, Italy).